Atmospheric Research 102 (2011) 311–319

Contents lists available at SciVerse ScienceDirect

Atmospheric Research

journal homepage: www.elsevier.com/locate/atmos

Ensemble prediction of Mediterranean high-impact events using potential vorticity perturbations. Part II: Adjoint-derived sensitivity zones

M. Vich *, R. Romero, V. Homar

Meteorology Group, Dpt. Física, Universitat de les Illes Balears, Palma de Mallorca, Spain

ARTICLE INFO

Article history:
Received 22 March 2011
Received in revised form 22 July 2011
Accepted 27 July 2011

Keywords:
Ensemble prediction system
PV perturbations
Adjoint model
Forecast verification
Mediterranean cyclones

ABSTRACT

In Part I of this work, an ensemble prediction system (EPS) based on different combinations of model physical parameterizations was compared against another ensemble based on perturbing initial and boundary conditions through the Potential Vorticity (PV) field. This comparison was done for western Mediterranean cyclonic situations associated with high-impact weather phenomena such as heavy rain and showed a better performance of the PV-perturbed ensemble over the more traditional multiphysics approach. The current study extends the comparison to another ensemble based on perturbing initial and boundary conditions through the PV field but guided by the MM5 adjoint derived sensitivity zones (PV-adjoint) instead of by the three-dimensional PV features showing intense values and gradients as was done in Part I (PV-gradient).

The PV-adjoint and PV-gradient EPSs perturb specific areas of the cyclonic development using a PV error climatology that typifies PV errors in the initial and boundary conditions to provide the appropriate error range. The non-hydrostatic MM5 mesoscale model nested in the ECMWF forecast fields is used to provide all predictions.

For the studied cases, 19 cyclonic events associated with heavy rain, the verification results show that both PV-perturbed are skillful, the PV-gradient being the best. Therefore, for our testbed, the extra computational cost of running the MM5 adjoint model does not provide a significant ensemble skill improvement.

1. Introduction

The intense cyclones and heavy rain events typical of the western Mediterranean region (Reiter, 1975; Meteorologial Office, 1962; Jansà et al., 2001) often have a high socio-economic impact on the coastal countries (Llasat and Sempere-Torres, 2001; Llasat et al., 2010). To succeed in preventing and reducing the damages caused by these events, their study and prediction is crucial. The first part of this study (Vich et al., (2011), hereafter referred to as Part I) showed an improvement in the prediction skill of these high-impact weather events for an ensemble prediction system based on perturbing the model initial and boundary conditions over another one based on varying physical parameterization schemes. Hence the purpose of this study is to develop an additional EPS also based on perturbing the model initial and boundary conditions to test whether a further improvement in the quality of the probabilistic forecasts is possible.

Nowadays the concept of building an EPS perturbing the initial state is extended and it has more than proved its value. In fact this technique has been implemented operationally since the 1990s in different meteorological centers, such as the National Centers for Environmental Prediction (NCEP; (Toth and Kalnay, 1997)), the European Center for Medium-Range Weather Forecasts (ECMWF; (Palmer et al., 1992; Molteni et al., 1996)) and Meteorological Service of Canada (MSC; (Pellerin et al., 2003)) to cite a few. Although this technique has been widely implemented in Global EPS with very good results, the transition to a Local EPS presents difficulties and is yet to be

* Corresponding author at: Dpt. Física, Universitat de les Illes Balears, Cra. de Valldemossa, km 7.5, Palma de Mallorca, 07122, Illes Balears, Spain. Tel.: +34 971172536; fax: +34 971173426.
E-mail address: mar.vich@uib.es (M. Vich).

0169-8095/$ – see front matter © 2011 Elsevier B.V. All rights reserved.
doi:10.1016/j.atmosres.2011.07.016

defined unequivocally (e.g. Torn et al. (2006)). A more detailed review of initial condition perturbations and physical parameterization scheme techniques used in different meteorological centers, as well as some approaches on dealing with Limited Area Models (LAMs) lateral bounding forcing can be found in Part I, Warner et al., (1997), Eckel and Mass, (2005), Torn and Hakim, (2008) or Stensrud et al., (2009), among others.

In this study the perturbations are introduced into the initial and boundary potential vorticity field and propagated in the temperature and wind fields using a PV inversion algorithm. Perturbing the boundary conditions prevents the ensemble from losing variance as lead time increases (Nutter et al., 2004a; Nutter et al., 2004b). The used PV inversion technique links the wind fields to the temperature field through the mass-wind balance condition derived by Charney, (1955). Previous studies have already highlighted the sensitivity of cyclones and associated high-impact weather to PV perturbations (e.g. (Huo et al., 1999; Romero, 2008; Argence et al., 2008) and Part I). Perturbations in the initial conditions are shown to be crucial for the accurate simulation of severe convective events over the western Mediterranean (Cohuet et al., 2011).

The *PV-gradient* ensemble developed in Part I perturbs the PV field along the zones of the three-dimensional PV structure presenting the local most intense values and gradients of the field, while the *PV-adjoint* ensemble developed in this part of the study introduces the perturbations over the MM5 adjoint model calculated sensitivity zones. The PV-adjoint EPS takes advantage of the main application of an adjoint model: sensitivity analysis that determines the sensitivity of a particular forecast feature of interest to the initial condition. Formally, an adjoint model is defined as the transposition of a linear operator that is constructed tangent to the phase space trajectory that is followed by the forward nonlinear deterministic forecast. This tangent linear approximation can be affected by the time span of the adjoint run. The longer the evolution analyzed, the farther away from a linear evolution the perturbations evolve in the nonlinear model. The linear assumption for our numerical setup is valid for smooth integrated response functions defined at lead times up to 48 h, while decreasing to 24 h when diabatic processes significantly affect the response function (Homar and Stensrud, 2004). Also, the response function definition is critical since a response function highly influenced by nonlinear forecasted features, e.g. rain, may severely constrain the tangent linear approximation. In a study like ours, focused on the rainfall associated with intense cyclones, a response function involving a precursor of larger-scale dynamic feature like the intensity of a cyclone (the vertical component of the relative vorticity near the surface) allows us to circumvent the mentioned limitation in the response function definition without compromising the objective of the adjoint calculations (see Errico, (1997) for a more extensive review of adjoint models).

Following Homar and Stensrud, (2008) that classifies a sensitivity estimation as *objective* if it is based on the tangent linear and adjoint models, and *subjective* if it is based on human interpretation of the atmospheric fields and the links between the chosen forecast aspect and the initial structures as derived from the conceptual models, each ensemble can be tagged accordingly, the PV-gradient as subjective and the PV-adjoint as objective. Our comparison study aims to explore the advantages or disadvantages of using an objective method like MM5 adjoint model instead of the conceptual model that links the Mediterranean cyclogenesis to an upper-level precursor PV anomaly, the basis of the PV-gradient ensemble.

The evaluation of the ensembles is done over the same collection of 19 MEDEX[1] cyclones of Part I. This trial set is representative of the kind of events that this study targets: cyclones producing floods and strong winds over the western Mediterranean. The heavy rain associated with this kind of event awakes the interest of the public so, even though the precipitation field is hard to predict and verify due to its complex nature, it is the subject of our verification. Several verification scores and indices (i.e. Bias, ROC and Rank Histogram, among others) are used in testing the performance of both EPSs.

This paper describes the building and evaluation of the two above mentioned ensemble prediction systems. A description of the ensembles generation methodology and implementation is given in Section 2. Section 3 presents the ensembles verification procedure and results. Some concluding remarks are found in Section 4.

2. Ensemble prediction systems design

The building of the PV-adjoint ensemble is analogous to the construction of the PV-gradient EPS, except for the criterion used to create the PV perturbations. Both ensembles are made up of 13 members (12 perturbed members plus a non-perturbed) using the same MM5 configuration to run all the simulations as detailed in Part I. Briefly, the model physical parameterization set consists of the explicit moisture scheme of Reisner graupel (Reisner et al., 1998), the cumulus parameterization scheme of Kain-Fritsch 2 (Kain, 2004), the PBL scheme of MRF (Troen and Mahrt, 1986; Hong and Pan, 1996), the cloud radiation scheme of Dudhia, (1989) and the five-layer soil model described in Dudhia, (1996), and the simulation domain (Fig. 3) is defined over a grid mesh made up of 30 sigma levels on the vertical and 120×120 nodes with a 22.5 km resolution on the horizontal. The verification framework consists of a 56-day period from a collection of 19 MEDEX episodes between September 1996 and October 2002 and the climatological rain gauge network maintained by AEMET (Agencia Estatal de Meteorología - Spanish Weather Service), which provides 24 h accumulated precipitation from 06 UTC to 06 UTC daily (see Part I for a more detailed description).

2.1. Perturbation technique

Our study is focused on high impact weather in a limited area, so instead of using a more standard technique, an approach that focuses on perturbing the PV field is proposed, exploiting the well-known connection between PV structures and our target (cyclones). For example, Beare et al., (2003) stated that cyclogenesis is sensitive to PV structures at different spatial scales, Snyder et al. (2003) found a strong relation between the reference state of the PV field and the evolution of PV perturbations, while Plu and Arbogast (2005) pointed at the likelihood of replicating the system variability modifying the PV coherent structures present in the analyses.

[1] MEDEX is a Mediterranean experiment on cyclones that produce high impact weather in the Mediterranean, a project endorsed by WMO (*http://medex.aemet.uib.es*) and currently under the THORPEX organization.

The PV-gradient and PV-adjoint ensembles are both based on the idea of perturbing the initial and boundary conditions through the PV field differing only in the criteria that locates the perturbed zones. The PV-gradient uses the zones of most intense values and gradients of the PV field as guidance. As detailed in Part I, this choice adopts these zones as the most sensitive zones (Garcies and Homar, 2009; Romero et al. 2006) of the subsequent atmospheric evolution, like the cyclogenesis process that occurs over the western Mediterranean. On the other hand, the PV-adjoint uses the PV sensitivity field calculated with the MM5 adjoint model, assuming these objectively-obtained zones are the most sensitive areas of the later cyclonic evolution. The MM5 adjoint sensitivity field has already proved its value in computing sensitivity areas of intense Mediterranean cyclones, as several previous studies maintain (e.g. (Homar and Stensrud, 2004; Homar et al., 2006; Homar and Stensrud, 2008), among others). In this study, the MM5 adjoint simulation timespan is 24 h. which assures that the tangent linear assumption made by the adjoint run is valid. The linear assumption can also be hampered if nonlinear

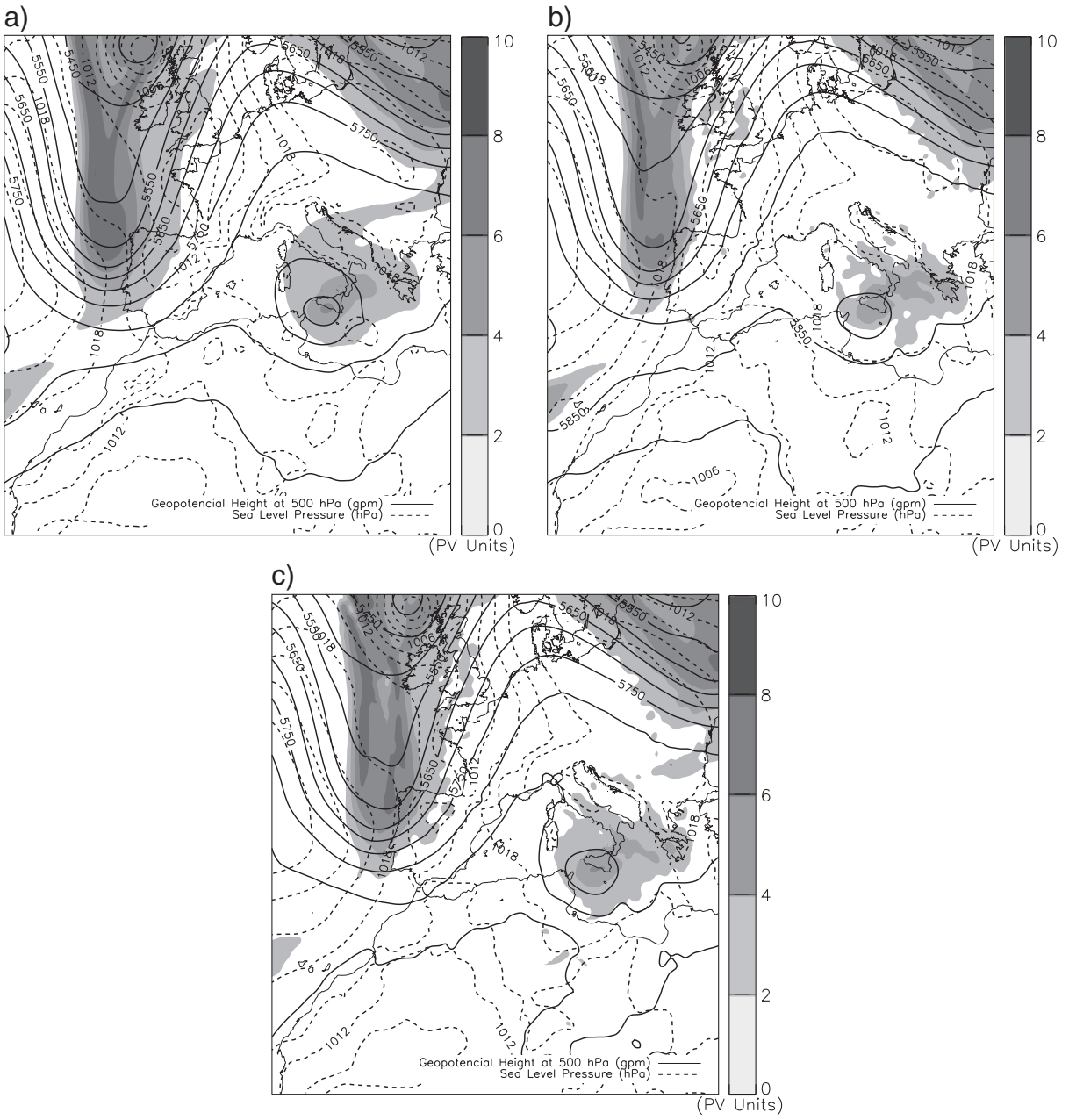

Fig. 1. Synoptic situation for 9 June 2000 at 00 UTC. a) Non-perturbed initial conditions (ECMWF 24 h forecast), b) PV-gradient and c) PV-adjoint ensemble member perturbed initial conditions for a randomly-chosen ensemble member. Note that the PV-gradient ensemble member is different than the one displayed in Fig. 2 of Part I. Geopotential height (continuous line, in gpm) at 500 hPa, sea level pressure (dashed line, in hPa), and potential vorticity on the 330 K surface (shaded contours, in PV units).

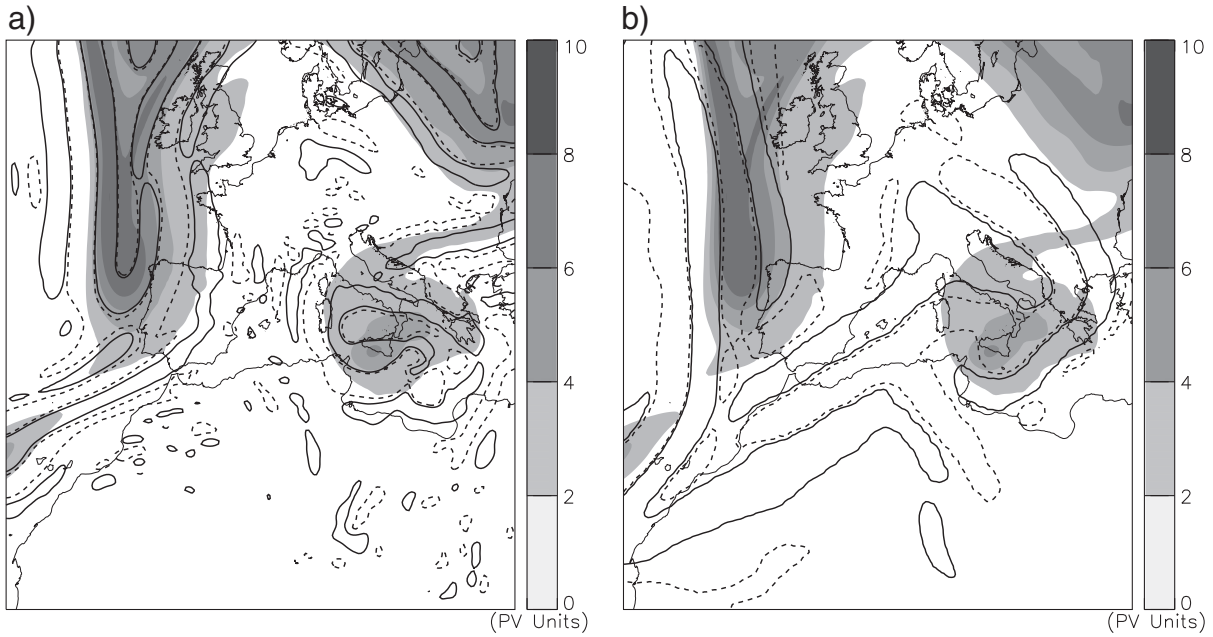

Fig. 2. a) PV-gradient EPS and b) PV-adjoint ensemble horizontal section of perturbation volumes at 300 hPa, solid line positive value (guidance field values over the threshold) and dashed line negative value (guidance field values below the negative of the threshold). As shaded contours in PV units, unperturbed potential vorticity field on 330 K surface.

processes are dominant, so the explicit nonlinear processes present in a high resolution adjoint run may lead to unreliable sensitivity results (Homar and Stensrud, 2004). A 90 km horizontal resolution for the adjoint run resolves well the dynamic features of interest (MEDEX cyclones) and does not diminish the physical capabilities of the adjoint while also keeping the computation cost low. Therefore, the simulation domain is defined as a 90 km resolution horizontal grid mesh with 86×120 nodes, centered at 41° latitude and 3° longitude. The vertical grid mesh is defined by 30 sigma levels. The physical parameterizations of adjoint models are not as well resolved as in the standard model version since they are based on a linear version of the model equations, so in this study the adjoint configuration considers a dry atmosphere to assure the Courant–Friedrichs–Lewy condition (CFL condition) with our available computational resources for all the needed MM5 adjoint runs, one run per day of study.

2.2. Practical implementation

As detailed in Part I, in the PV-gradient building procedure, the guidance field is defined by the difference between the three-dimensional PV field and a highly smoothed version of itself, thus highlighting the most intense values and gradients. On the other hand, in the PV-adjoint procedure the guidance field corresponds to the PV sensitivity field obtained with the MM5 adjoint model. Once the guidance field is known, the following generation stages for both ensembles are the same. A threshold is then defined as the average of the guidance field over the whole domain, in absolute value. The three-dimensional regions where the perturbations are introduced are then defined by the 3D regions where the guidance field exceeds, in absolute value, the threshold. On each of these volumes the intensity – both magnitude and sign – and displacement perturbations are assigned randomly accordingly to the PV error climatology.[2] On the other hand, the displacement direction perturbation is assigned using the same randomly chosen value to all volumes to avoid discontinuities in the perturbed PV field. After perturbing, the difference between the original and perturbed balanced fields (obtained applying the PV inversion technique) is added to the non-perturbed, mass and wind fields, to produce the initial and boundary conditions of the corresponding ensemble member.

To illustrate the different various steps of the perturbing procedure the 9–10 June 2000 case study is presented next, see Part I for a more detailed description. Briefly, the northeastern part of the Iberian Peninsula was affected by a quasi-stationary convective system associated with heavy precipitation causing severe floods. The synoptic situation on 9th June 2000 at 00 UTC is shown in Fig. 1a. A more detailed dynamic description of the event can be found in Martín et al., (2007).

Fig. 2 shows a horizontal section at 300 hPa of the perturbation volumes. The PV-gradient zones follow closely the structure of the upper-level trough as one would expect given its definition (Fig. 2a), while the PV-adjoint ones highlight different regions but also contain the upper-level trough regions (Fig. 2b).

Fig. 1 gathers the results of the perturbing technique showing the visible differences on the PV, geopotential and sea level pressure fields between the non-perturbed, the PV-gradient and PV-adjoint perturbed initial conditions. The MM5 model is initialized and forced with each perturbed initial condition and used to run the 54 h forecasts. Fig. 3 shows the 30–54 h forecast accumulated rainfall mean and standard deviation (STD) of each

[2] PV error climatology derived in Part I to assure that the perturbations are consistent with PV field uncertainty range.

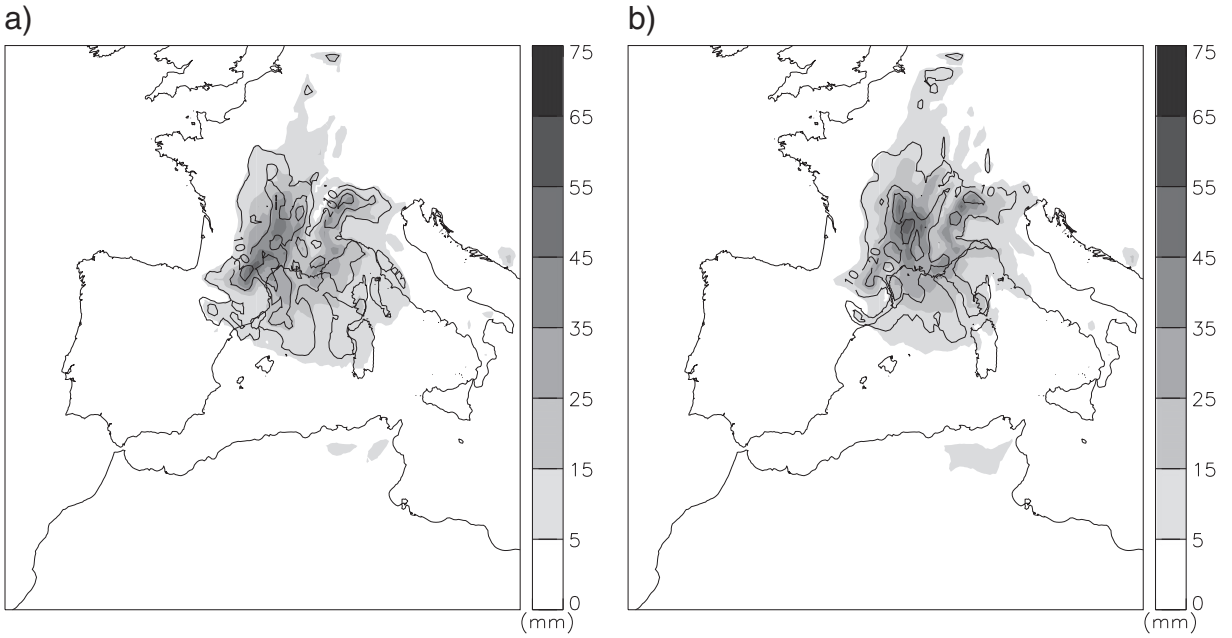

Fig. 3. Ensemble mean (shaded contours, in mm) and ensemble standard deviation (solid line, in mm at 10 mm intervals) for the 24 h accumulated precipitation over the forecasted region (from 10 to 11 June 2000 at 06 UTC). a) PV-gradient ensemble and b) PV-adjoint EPS.

13-member ensemble. The PV-gradient ensemble presents the highest rainfall values located farther south than in the PV-adjoint results and with a more meridionally elongated pattern across France, while both STD fields present relative maxim over the highest rainfall values. An extensive examination of the performance of each ensemble is done in the following section.

3. Verification results

An evaluation of the predictive skill of each EPS is done using probabilistic scores and indices, assuming each deterministic forecast (ensemble member) as an independent realization of the same underlying process. The verification is done for the 24 h accumulated precipitation period corresponding to the second day of simulation and addresses the general performance of the ensembles, not a unique observation threshold. Therefore, nine rainfall amount thresholds (0, 2, 5, 10, 20, 30, 50, 100 and 150 mm) have been defined as observed events.

Traditional verification techniques are affected by the difficulties derived from matching the forecast and the verifying data (Mass et al., 2002), a procedure especially hard on our verification field, precipitation, due to its discontinuous nature both in space and time. During the last few years, several

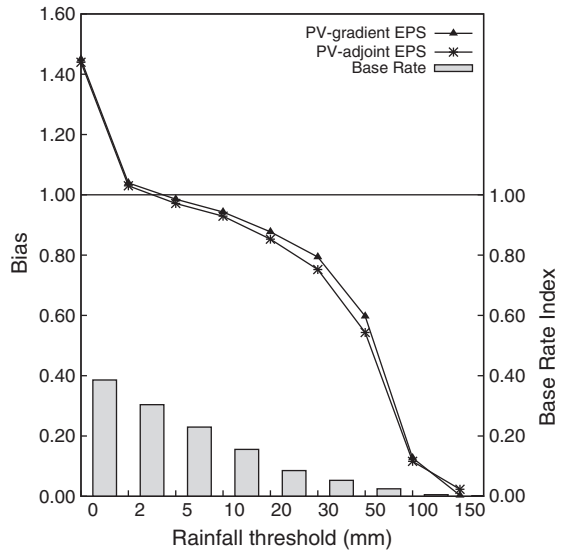

Fig. 4. Frequency bias for the PV-gradient and PV-adjoint ensembles, as function of different rainfall thresholds. The base rate index shown by the histogram represents the observed event probability (the sample size is 109,276).

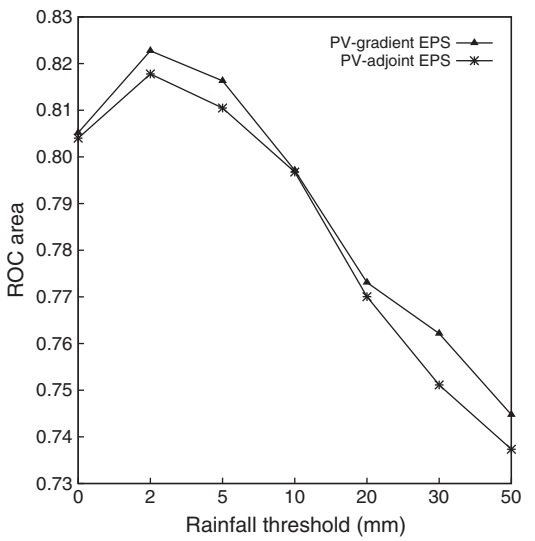

Fig. 5. ROC area for the PV-gradient and PV-adjoint ensembles, as function of different rainfall event thresholds.

techniques have been developed to handle this issue through spatial oriented verification instead of point-to-point techniques (see Casati et al., 2008 and Gilleland et al., 2009 for reviews). Albeit these methods are more advanced and precipitation oriented, at their current development stage, they rely on observations defined on a dense regular network (like radar or satellite) over a spatial domain, which is not always a possibility. On the other hand, the point-to-point techniques can function on sparse networks like the observational rain gauge network available for this study.

A description of each verification measure used here can be found in Part I, and a more thorough discussion in Jolliffe and Stephenson (2003) and Wilks (1995), for example. Since the Bias score compares the forecast and observed event frequencies, Fig. 4 shows a slightly better performance of the PV-gradient ensemble over the PV-adjoint system considering that both EPSs overpredict (bias>1) rainfall amounts less than 5 mm while they underpredict (bias<1) the larger rainfall amounts. Between 2 and 10 mm thresholds both EPSs are almost unbiased. The fast bias decay towards zero for greater thresholds, above 50 mm, is most probably due to a sample problem as indicated by the rapid decrease in the number of events of extreme precipitation values (Base Rate in Fig. 4). It may also be due to the difficulties of the EPSs to forecast extreme precipitation values while running over a 22.5 km horizontal resolution domain. Therefore, our verification procedure focuses on the thresholds ranging from 0 to 50 mm due to the lack of statistical significance outside this range and the low capability of mesoscale models to handle extreme precipitation forecasts.

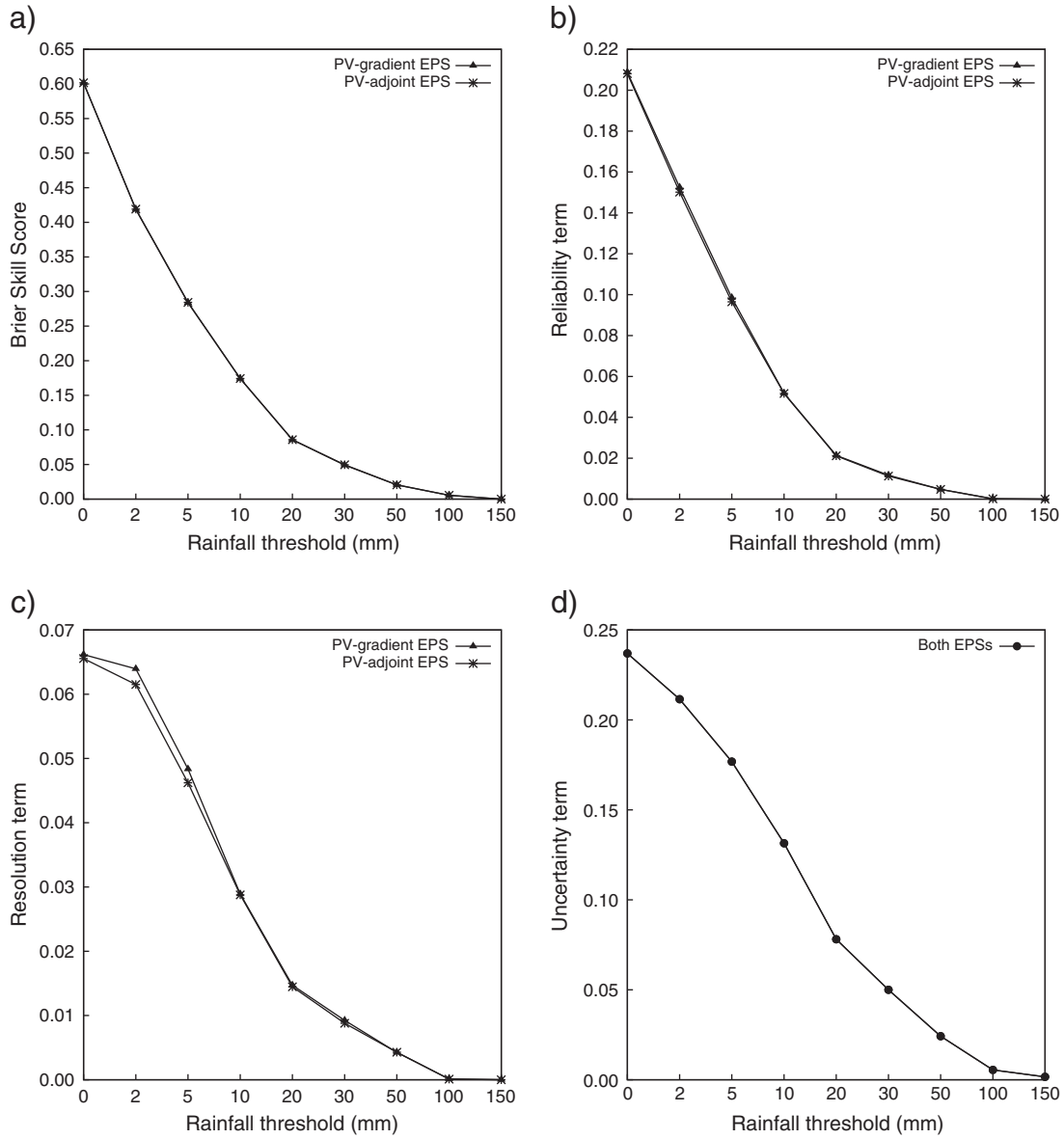

Fig. 6. Brier Skill Score and the Brier Score three components for the PV-gradient and PV-adjoint ensembles, shown as function of different rainfall event thresholds. a) Brier Skill Score, b) Brier Score Reliability term, c) Brier Score Resolution term, and d) Brier Score Uncertainty term (only depends on the observations).

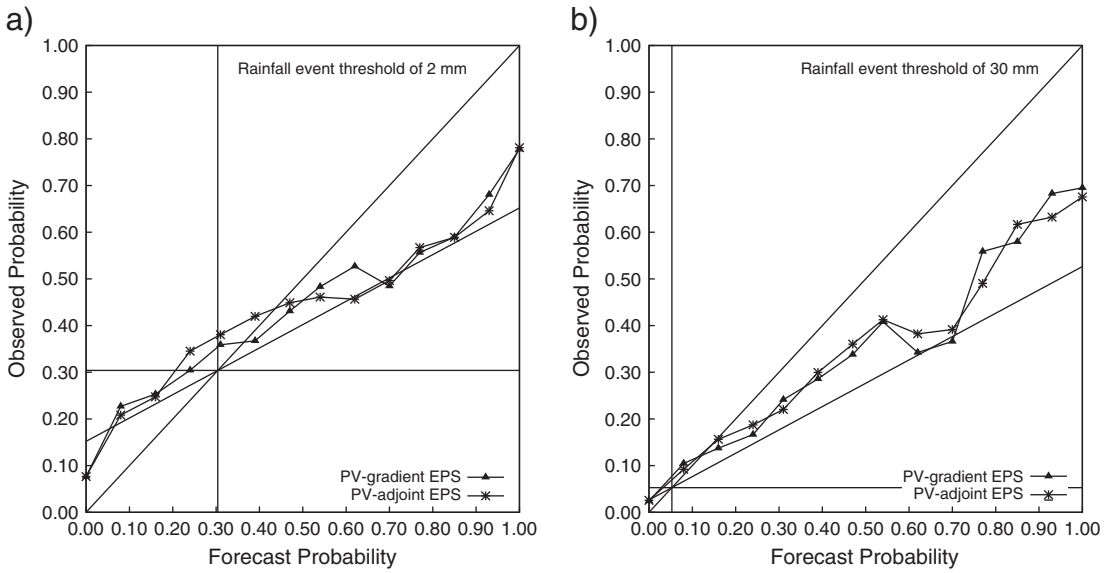

Fig. 7. Attribute diagrams for the PV-gradient and PV-adjoint ensembles, for a) 2 mm and b) 30 mm rainfall event thresholds. The perfect score is represented by a curve that matches the diagonal. The vertical and horizontal lines represent the no-resolution, also known as the climatological frequency of the event, and the 0.5 slope that crosses the no-resolution and perfect score lines represents the no-skill line.

The ROC curve (Mason, 1982), a graph of probability of detection against probability of false detection, indicates the ability of the forecast to discriminate between events and non-events. The area under the ROC curve (ROC area) is also a good indication of discriminating skill of the system, in fact an area of 0.5 indicates no skill above random fit and 1 a perfect skill. The ROC areas obtained for both ensembles (Fig. 5) are very skillful since all forecasts lie well above 0.7, the threshold established by Stensrud and Yussouf, (2007) which indicates the usefulness of the forecasting system. Both EPSs exhibit good results for all rainfall thresholds presenting their maximum value at 2 mm. The PV-gradient ensemble shows better skill than the PV-adjoint for all the rainfall thresholds, except for the 10 mm where their skill is similar.

The Brier Score (Brier, 1950) indicates the magnitude of the probability forecast errors, while the Brier Skill Score measures the difference between the score for the forecast and the score for the unskilled standard forecast, normalized by the total possible improvement that can be achieved. The Brier Score can also be decomposed into the sum of three individual parts related to reliability, resolution and the underlying uncertainty of the observations (Murphy, 1973). Fig. 6 shows that the Brier Skill Score is almost the same for both EPSs, while the BS terms show different behaviors depending on the EPS. Both EPSs

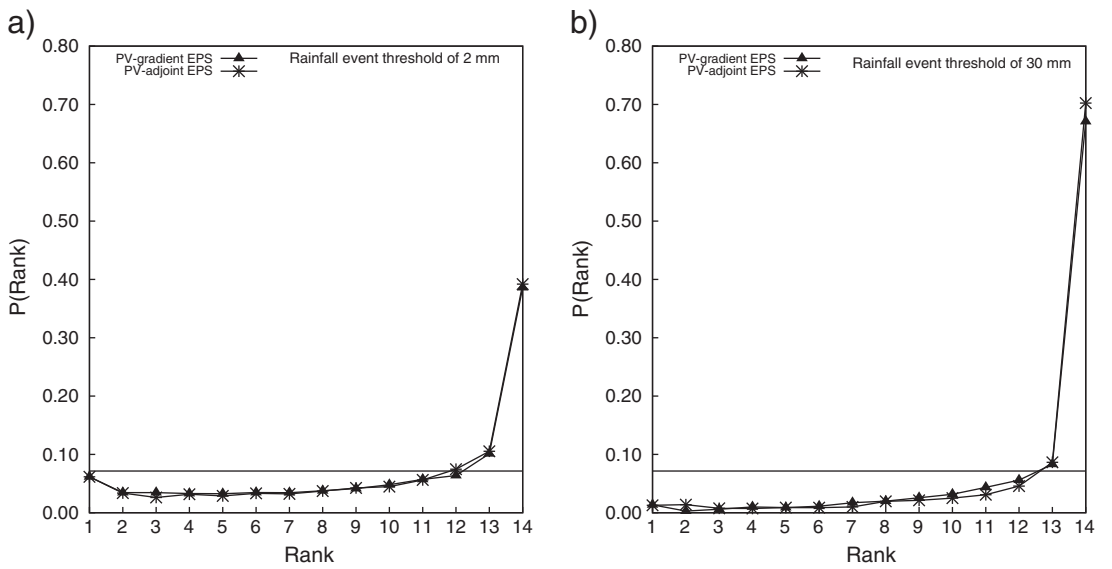

Fig. 8. Rank histograms for the PV-gradient and PV-adjoint ensembles, for a) 2 mm and b) 30 mm rainfall event thresholds. The horizontal line or flat histogram represents the perfect score.

present good skill for low rainfall thresholds that decreases as the rainfall threshold increases. As the BS uncertainty term exclusively depends on the observation uncertainties and not on the forecast, the results for all the EPSs are identical as they share the same observational database. The near coincidence of both EPSs on the BSS are due to the BS reliability and BS resolution terms, two terms of opposite signs, that almost compensate each other in the total score. The BS reliability is almost the same for both ensembles (indistinguishable in the graph) indicating that both ensembles present very similar reliability skill, while the BS resolution term is slightly different between ensembles but not enough to show a meaningful difference in how the different forecasted events are classified by the forecast system, even though the PV-gradient ensemble slightly outperforms the PV-adjoint.

The attribute diagrams illustrate the correspondence between the predicted probabilities of an event and its observed frequencies. Fig. 7 gathers the results for the 2 and 30 mm rainfall thresholds and states how the skill of both ensembles decreases as the threshold increases. In spite of this skill decrease, the curves remain inside the skill region. Even though both ensembles lay inside the skill region, both ensembles exhibit a tendency to underforecast the Observed Probability for low values of Forecast Probability and overforecast it for high values, indicating a conditional bias. Nevertheless, the PV-gradient is closer globally to the perfect score than the PV-adjoint.

Another verification measure is the rank histogram (Talagrand et al., 1997) that evaluates if the spread of the ensemble truly captures observations variability. All rank histograms (Fig. 8) present a U-shaped form combined with a pronounced right-asymmetric profile due to an excessive population within the extreme rank, revealing that the ensembles clearly underestimate the higher precipitation values and slightly overestimate the lower precipitation values (an extended discussion on rank histogram interpretation can be found in Hamill, (2001)). This behavior agrees with the bias results (Fig. 4) which also show overprediction for lower thresholds and underprediction for higher. Once again, the PV-gradient ensemble shows slightly better skill than the PV-adjoint.

4. Concluding remarks and future outlook

The performance of two different EPSs has been evaluated using a thorough verification procedure. Considering that the aim of this study is to improve the short-range numerical forecasts of cyclones associated with heavy rain events in the western Mediterranean, the verification setup is focused on the 24 h accumulated precipitation field; a field observed over non gridded networks and highly discontinuous in both space and time that makes the evaluation harder and more demanding. In addition, the study also deals with extreme events which are difficult to predict in nature and rare by definition.

Both ensembles are built using a single variable (PV) to define perturbations combined with the PV Inversion Technique, keeping the method simple while ensuring modifications of all the meteorological fields without compromising the mass-wind balance. The only difference between both EPSs lies in where the perturbations are introduced. The PV-gradient ensemble introduces the perturbations in the areas corresponding to the PV zones of most intense values and gradients (in essence a subjective choice based on our experience) while the PV-adjoint does it in the MM5 adjoint model calculated sensitivity zones (an objective method).

The high computational cost of the PV-adjoint ensemble (which implies running the MM5 adjoint model for each simulation day) versus the low cost of the PV-gradient is not compensated later in ensemble skill. Even though both EPSs are skillful and present a more than adequate performance, the results obtained by the PV-gradient ensemble are generally better than those obtained by the PV-adjoint EPS. Thus, the PV-gradient ensemble is proved to be a more profitable strategy than the PV-adjoint EPS, which is also useful but computationally more expensive for our testbed. This result is in agreement with Homar and Stensrud's (2008) results, which stated that for intense cyclogenesis over the western Mediterranean, adjoint-estimated sensitivity is comparable or slightly inferior to subjective (gradient and human) sensitivity estimates.

In view of these results, the future work should continue to explore additional ensemble generation methods based upon perturbing the initial and boundary conditions through the PV field. Moreover, the perturbation volumes should be guided by a method centered on the precursor upper-level trough characteristic of the mid-latitude cyclonic situations as in our first method, since the presented results hint that these are the most fruitful dynamical structures.

Acknowledgments

Support from PhD grant BES-2006-14044 and MEDICANES CGL2008-01271/CLI project, both from the Spanish *Ministerio de Ciencia e Innovación*, is acknowledged. Precipitation data and access to ECMWF database was provided by AEMET.

References

Argence, S., Lambert, D., Richard, E., Chaboureau, J.P., Söhne, N., 2008. Impact of initial condition uncertainties on the predictability of heavy rainfall in the Mediterranean: a case-study. Q. J. R. Meteorol. Soc. 134, 1775–1788.

Beare, R., Thorpe, A., White, A., 2003. The predictability of extratropical cyclones: nonlinear sensitivity to localized potential vorticity perturbations. Q. J. R. Meteorol. Soc. 129, 219–237.

Brier, G.W., 1950. Verification of forecasts expressed in terms of probabilities. Mon. Wea. Rev. 78, 1–3.

Casati, B., Wilson, L., Stephenson, D., Nurmi, P., Ghelli, A., Pocernich, M., Damrath, U., Ebert, E., Brown, B., Mason, S., 2008. Forecast verification: current status and future directions. Meteor. Appl. 15, 3–8.

Charney, J.G., 1955. The use of primitive equation of motion in numerical prediction. Tellus 7, 22–26.

Cohuet, J.B., Romero, R., Homar, V., Ducrocq, V., Ramis, C., 2011. Initiation of a severe thunderstorm over the Mediterranean Sea. Atmos. Res. 100, 603–620. doi:10.1016/j.atmosres.2010.11.002.

Dudhia, J., 1989. Numerical study of convection observed during the winter monsoon expriment using a mesoscale two-dimensional model. J. Atmos. Sci. 46, 3077–3107. doi:10.1175/1520-0469(1989) 046(3077:NSOCOD)2.0.CO;2.

Dudhia, J., 1996. A multi-layer soil temperature model for mm5. Preprints from the Sixth PSU/NCAR Mesoscale Model Users' Workshop. http://www.mmm.ucar.edu/mm5/lsm/soil.pdf. 22–24.

Eckel, F., Mass, C., 2005. Aspects of effective mesoscale, short-range ensemble forecasting. Wea. Forecasting. 20, 328–350.

Errico, R.M., 1997. What is an adjoint model? Bull. Amer. Meteor. Soc. 78, 2577–2591.

Garcies, L., Homar, V., 2009. Ensemble sensitivities of the real atmosphere: Application to Mediterranean intense cyclones. Tellus A, In Press.

Gilleland, E., Ahijevych, D., Brown, B., Casati, B., Ebert, E., 2009. Intercomparison of spatial forecast verification methods. Wea. Forecasting. 24, 1416–1430.

Hamill, H.C., 2001. Interpretation of rank histograms for verifying ensemble forecasts. Mon. Wea. Rev. 129, 550–560.
Homar, V., Stensrud, D.J., 2004. Sensitivities of an intense mediterranean cyclone: analysis and validation. Q. J. R. Meteorol. Soc. 130, 2519–2540.
Homar, V., Stensrud, D.J., 2008. Subjective versus objective sensitivity estimates: application to a North African cyclogenesis. Tellus A 60, 1064–1078. doi:10.1111/j.1600-0870.2008.00353.x.
Homar, V., Stensrud, D.J., Levit, J.J., Bright, D.R., 2006. Value of human-generated perturbations in short-range ensemble forecasts of severe weather. Wea. Forecasting 21, 347–363.
Hong, S.Y., Pan, H.L., 1996. Nonlocal boundary layer vertical diffusion in a medium-range forecast model. Mon. Wea. Rev. 124, 2322–2339.
Huo, Z., Zhang, D.L., Gyakum, J., 1999. Interaction of potential vorticity anomalies in extratropical cyclogenesis. Part I: static piecewise inversion. Mon. Wea. Rev. 127, 2546–2560.
Jansà, A., Genovés, A., Picornell, M.A., Campins, J., Riosalido, R., Carretero, O., 2001. Western Mediterranean cyclones and heavy rain. Part 2: statistical approach. Meteor. Appl. 8, 43–56.
Jolliffe, I.T., Stephenson, D.B., 2003. Forecast Verification: A Practioner's Guide in Atmospheric Science. John Wiley and Sons.
Kain, J.S., 2004. The Kain-Fritsch convective parameterization: an update. J. Appl. Meteor. 43, 170–181.
Llasat, M., Sempere-Torres, D., 2001. Heavy rains and floods in west mediterranean areas: a climatic feature. Geophysical Research Abstr acts, 3. European Geophysical Society.
Llasat, M., Llasat-Botija, M., Prat, M., Porcú, F., Price, C., Mugnai, A., Lagouvardos, K., Kotroni, V., Katsanos, D., Michaelides, S., Yair, Y., Savvidou, K., Nicolaides, K., 2010. High-impact floods and flash floods in Mediterranean countries: the FLASH preliminary database. Adv. Geosci. 23, 1–9.
Martín, A., Romero, R., Homar, V., De Luque, A., Alonso, S., Rigo, T., Llasat, M.C., 2007. Sensitivities of a flash flood event over Catalonia: a numerical analysis. Mon. Wea. Rev. 135, 651–669.
Mason, I., 1982. A model for assessment of weather forecasts. Austr. Meteor. Mag. 30, 291–303.
Mass, C., Ovens, D., Westrick, K., Colle, B., 2002. Does increasing horitzontal resolution produce more skillful forecasts? Bull. Amer. Meteor. Soc. 83, 407–430.
Meteorologial Office, 1962. Weather in the Mediterranean. Air Ministry, Vol.1. 362 pp.
Molteni, F., Buizza, R., Palmer, T.N., Petroliagis, T., 1996. The ECMWF ensemble prediction system: methodology and validation. Q. J. R. Meteorol. Soc. 122, 73–119.
Murphy, A., 1973. A new vector partition of the probability score. J. Appl. Meteor. 12, 534–537.
Nutter, P., Stensrud, D., Xue, M., 2004a. Effects of coarsely resolved and temporally interpolated lateral boundary conditions on the dispersion of limited-area ensemble forecasts. Mon. Wea. Rev. 132, 2358–2377.
Nutter, P., Xue, M., Stensrud, D., 2004b. Application of lateral boundary condition perturbations to help restore dispersion in limited-area ensemble forecasts. Mon. Wea. Rev. 132, 2378–2390.
Palmer, F., Molteni, F., Mureau, R., Buizza, P., Chapelet, P., Tribbia, J., 1992. Ensemble prediction. ECMWF Res. Dept. Tech. Memo. 188 45 pp..
Pellerin, G., Lefaivre, L., Houtekamer, P., Girard, C., 2003. Increasing the horitzontal resolution of ensemble forecasts at CMC. Nonlinear Proc. Geophys. 10, 463–468.
Plu, M., Arbogast, P., 2005. A cyclogenesis evolving into two distinct scenarios and its implications for short-term ensemble forecasting. Mon. Wea. Rev. 133, 2016–2029.
Reisner, J., Rasmussen, R., Bruintjes, R., 1998. Explicit forecasting of super-cooled liquid water in winter storms using the mm5 mesoscale model. Q. J. R. Meteorol. Soc. 124, 1071–1107. doi:10.1002/qj.49712454804.
Reiter, E., 1975. Handbook for Forecasters in the Mediterranean. Part 1: General Description of the Meteorological Processes. Naval Environmental Research Facility, Monterey, California.
Romero, R., 2008. A method for quantifying the impacts and interactions of potential-vorticity anomalies in extratropical cyclones. Q. J. R. Meteorol. Soc. 134, 385–402.
Romero, R., Martín, A., Homar, V., Alonso, S., Ramis, C., 2006. Predictability of prototype flash flood events in the western Mediterranean under uncertainties of the precursor upper-level disturbance: the HYDRO-PTIMET case studies. Adv. Geosci. 7, 55–63.
Snyder, C., Hamill, T., Trier, S., 2003. Linear evolution of error covariances in quasigeostrophic model. Mon. Wea. Rev. 131, 189–205.
Stensrud, D., Yussouf, N., 2007. Reliable probabilistic quantitative precipitation forecasts from a short-range ensemble forecasting system. Wea. Forecasting. 22, 3–17.
Stensrud, D.J., Yussouf, N., Dowell, D.C., Coniglio, M.C., 2009. Assimilating surface data into a mesoscale model ensemble: cold pool analyses from spring 2007. Atmos. Res. 93, 207–220. doi:10.1016/j.atmosres.2008.10.009.
Talagrand, O., Vautard, R., Strauss, B., 1997. Evaluation of Probabilistic Prediction Systems. ECMWF, pp. 1–25.
Torn, R., Hakim, G., 2008. Performance characteristics of a pseudo-operational ensemble Kalman filter. Mon. Wea. Rev. 136, 3947–3963.
Torn, R., Hakim, G., Snyder, C., 2006. Boundary conditions for limited-area ensemble Kalman filters. Mon. Wea. Rev. 134, 2490–2502.
Toth, Z., Kalnay, E., 1997. Ensemble forecasting at ncep and the breeding method. Mon. Wea. Rev. 125, 3297–3319.
Troen, I., Mahrt, L., 1986. A simple model of the atmospheric boundary layer: sensitivity to surface evaporation. Bound-Lay Meteorol. 37, 129–148.
Vich, M., Romero, R., Brooks, H., 2011. Ensemble prediction of Mediterranean high-impact events using potential vorticity perturbations. Part I: Comparison against the multiphysics approach. Atmos. Res. In Press.
Warner, T., Peterson, R., Treadon, R., 1997. A tutorial on lateral boundary conditions as a basic and potentially serious limitation to regional numerical weather prediction. Bull. Amer. Meteor. Soc. 78, 2599–2617.
Wilks, D., 1995. Statistical Methods in the Atmospheric Sciences: An Introduction. Academic. Press.